Dynamic fluctuations in ascending heart–to–brain modulations under mental stress elicitation

Diego Candia-Rivera [1*], Kian Norouzi [2,3], Thomas Zoëga Ramsøy [2,4] and Gaetano Valenza [1].

[1] Bioengineering and Robotics Research Center E. Piaggio & Department of Information Engineering, School of Engineering, University of Pisa, 56122, Pisa, Italy

[2] Neurons Inc., Department of Applied Neuroscience, Taastrup, Denmark.

[3] Faculty of Management, University of Tehran, Tehran, Iran.

[4] Faculty of Neuroscience, Singularity University, Santa Clara, CA, United States

* Corresponding author: diego.candia.r@ug.uchile.cl

Keywords

Brain–heart interplay, mental stress, physiological modeling, sympathovagal control

Abstract

Dynamical information exchange between central and autonomous nervous systems, as referred to functional brain–heart interplay, occurs during emotional and physical arousal. Nevertheless, the role of such a nervous-system-wise communication in mental stress is yet unknown. In this study, we estimate the causal and bidirectional neural modulations between EEG oscillations and peripheral sympathetic and parasympathetic activities using a recently proposed computational framework for a functional brain–heart interplay assessment, namely the sympatho-vagal synthetic data generation model. Mental stress is elicited in 37 healthy volunteers by increasing their cognitive demand throughout four tasks associated with increasing stress levels. Stress elicitation induced an increased variability in the directional heart–to–brain functional interplay, primarily originating from sympathetic activity targeting a wide range of EEG oscillations. These findings extend current knowledge on stress physiology, which referred to primarily a top-down neural dynamics. Our results suggest that mental stress involves dynamic and bidirectional neural interactions at a brain–body level, where bodily feedback may modulate the perceived stress caused by an increased cognitive demand. We conclude that directional brain–heart interplay measurements may provide suitable biomarkers for a quantitative stress assessment.

1. Introduction

Human physiology entails constant and dynamic adaptations in response to cognitive demand through homeostatic and allostatic mechanisms. From a holistic point of view, the physiological responses to cognitive load refer to "mental stress", which can be elicited by memory, arithmetic, and increased cognitive demand tasks (1). Physical stress involves the physiological responses triggered by homeostatic regulations to bodily conditions, emerging from physical exercise or environmental changes (e.g., temperature or atmospheric pressure) (1). Mental and physical stress encompass physiological responses from different brain structures, together with responses from peripheral systems (2). The neurophysiology of stress sets the hypothalamus as a central component, in which the paraventricular nucleus is the main integrator of stressors, activating systems such as the sympathetic-adreno-medullar and hypothalamus-pituitary-adrenal axes (3). The brain structures actively involved in stress responses include the prefrontal cortex (4) and the amygdala, whose activity is also associated with emotional processing (5). Prefrontal projections to the amygdala (6), as well as hippocampus projections to the amygdala and prefrontal cortex (7) are involved as well. Underlying stress mechanisms have also been captured in EEG studies, showing a high diversity of responses, including hemispheric changes in alpha power and wide-range variability in the EEG spectrum (8, 9).

The central autonomic network integrates the interoceptive and exteroceptive information to promote physiological and behavioral changes that allow adaption to ongoing challenges, including stress conditions (2, 10–12). Therefore, stress can significantly modulate autonomic activity, as previously reported in heart rate variability (13–17), skin conductance (17, 18), breathing rate (19), body temperature (20, 21) and blood pressure (13, 14, 17)– but also gastrointestinal (22, 23), endocrine (24) and immune responses (25). On the other hand, acute stress triggers concurrent fluctuations in heart rate variability and functional connectivity between central executive and default mode networks (26). Neural responses to heartbeats have been described as a potential indicator of stress, because of the correlations found with sympathetic indexes (17). Similarly with the correlations found between EEG power and autonomic indexes under mental stress (27).

Since stress conditions may induce emotional responses (28), physiological responses to stress (i.e., stress regulation) may be linked to physiological mechanisms of emotion regulation (29). Indeed, while cardiovascular dynamics are modulated by emotions processing (30, 31), modulation activity of the functional brain–heart interactions have been observed under thermal stress and thermoregulatory responses (21, 32), as well as emotional processing (33). Accordingly, cardiac interoceptive feedback seems actively involved under stressful conditions (34, 35), and a wider involvement of the functional brain–body axis in mental stress have already

been hypothesized (36). Nonetheless, the functional brain-body physiology associated with mental stress is yet unknown.

To overcome this limitation, this study aims to uncover the directional brain–heart interplay mechanisms involved in mental stress induced through visual stimulation and memory tasks. Specifically, we exploit our recently proposed Sympathovagal Synthetic Data Generation model (SV-SDG) (32) to uncover the mutual functional communication between cortical oscillations, as measured through EEG, and cardiac sympathetic/parasympathetic activities, estimated from heartbeat dynamics. The SV-SDG model provides time-varying estimates of the causal interplay between sympathetic/parasympathetic activities and EEG oscillations in a specific frequency band. The framework embeds a heartbeat generation model based on the estimation of sympathetic and parasympathetic activities from a Laguerre expansions of the heartbeat series (37).

2. Materials and methods

2.1 Dataset description

Data were gathered from 37 healthy participants (age median 30 years, age range 22–45 years, 20 males, 17 females) who underwent mental stress elicitation tasks. Participants were asked to sit comfortably and follow instructions on a screen. Recordings of physiological signals included EEG (9-channel, Biopac B-Alert) and one lead ECG, both sampled at 256 Hz.

This study was performed at Neurons Inc, Taastrup, Denmark, in accordance with the Declaration of Helsinki and followed the rules and laws of the Danish Data Protection Agency. Data protection policy also followed the European Union law of the General Data Protection Regulation, as well as the ethical regulations imposed by the Neuromarketing Science and Business Association, Article 6. Each person's biometric data, survey responses, and other types of data were anonymized and only contained the log number as the unique identifier. Personal information cannot be identified from the log number.

2.2 Experimental protocol

The stress induction protocol comprises four stressing conditions, including 1-minute rest and three different stress load tasks lasting 14 minutes approximately. The stressors were presented in the same order to all participants. The first stress load condition consisted in watching a documentary. The second stress load condition consisted in watching a documentary concurrently to performing a digit span task. The third stress load condition consisted in watching a documentary, performing the digit span task and the red box task. For each condition, participants were asked to report the stress level through a discrete scale from 1 to 7.

More specifically, the first five minutes of the documentary "The Reality of Van Life", Different Media © 2018, was projected onto a screen as first stressor (Figure 1A). The digit span task starts with a fixation cross for 1.5 s. Then, three digits are presented for 5 s, followed by a blank screen for 4 s. The participant is then asked to verbally state the three digits in up to 5 s (Figure 1B). The red box task, run in parallel to the digit span task (Figure 1C), starts with a fixation cross for 1.5 s. Then a red box (4x4 red and white box pattern) is presented for 3 s. Next, the three digits are presented for 5 s, followed by a blank screen for 4 s. Then the participant is asked to verbally state the three digits in up to 5 s. Consecutively, a red box is presented, and the participant is asked if the pattern matches to the previously presented one (yes or no answer).

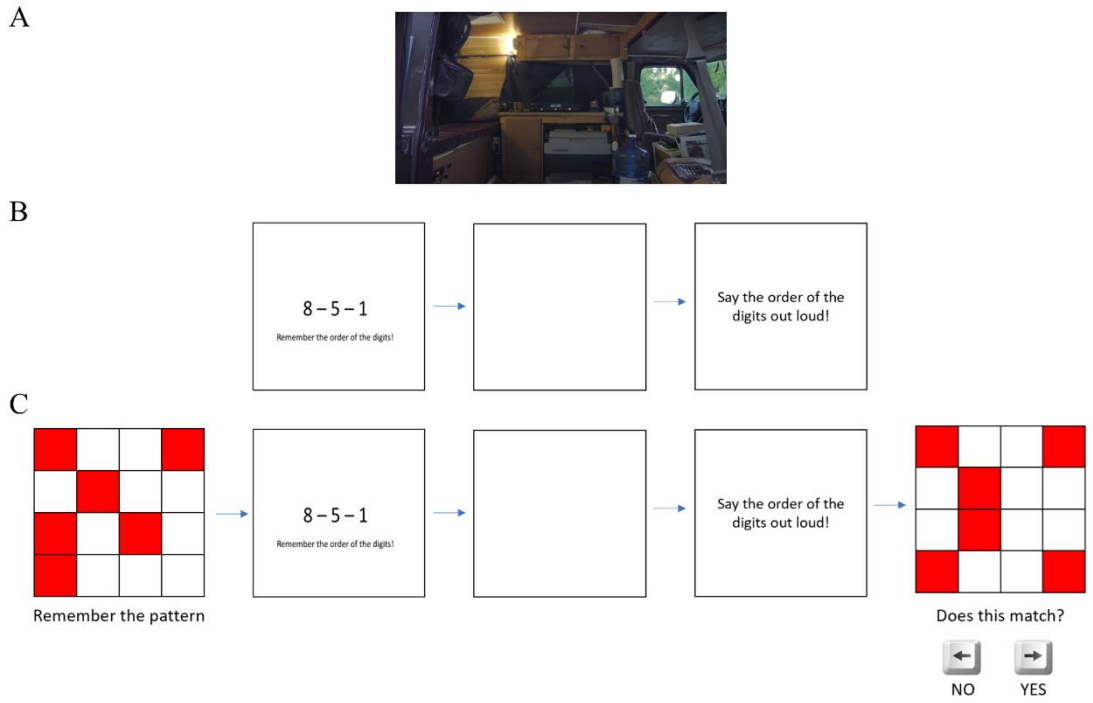

Figure 1. Experimental protocol. (A) Sample image from stress load condition 1, The Reality of Van Life, Different Media © 2018. (B) Sample image from stress load condition 2: digit span task. (C) Sample figure from stress load condition 3: digit span task + red box task.

2.3 EEG pre-processing

EEG data were pre-processed using MATLAB R2022a and Fieldtrip Toolbox (38). EEG data were bandpass filtered with a Butterworth filter of order 4, between 0.5 and 45 Hz. Large movement artifacts were visually identified and removed manually from independent component space and wavelet filtering. Consecutively, the Independent Component Analysis (ICA) was computed to visually recognize and reject the eye movements and cardiac-field artifacts from the EEG data. One lead ECG was included as an additional input to the ICA to enhance the process of finding cardiac artifacts. Once the ICA components with eye movements and cardiac artifacts were visually identified, they were removed to reconstruct the EEG series. Channels were re-referenced using a common average, which is the most appropriate for a brain–heart interplay estimations (39).

The EEG spectrogram was computed using the short-time Fourier transform with a Hanning taper. Calculations were performed through a sliding time window of 2 seconds with a 50% overlap, resulting in a spectrogram resolution of 1 second and 0.5 Hz. Then, time series were

integrated within five frequency bands (delta: 1-4 Hz, theta: 4-8 Hz, alpha: 8-12 Hz, beta: 12-30 Hz, gamma: 30-45 Hz).

2.4 ECG data processing

ECG time series were bandpass filtered using a Butterworth filter of order 4, between 0.5 and 45 Hz. The R-peaks from the QRS waves are detected in a procedure based on template-matching method (39). All the detected peaks were visually inspected over the original ECG, along with the inter-beat intervals histogram. Manual corrections were performed where needed and guided from the automatic detection of ectopic beats (40).

2.5 Functional brain–heart interplay assessment

The Sympathovagal Synthetic Data Generation model (SV-SDG) provides time-variant estimates of the bidirectional functional coupling between heartbeat and brain components. The model uses the estimation of sympathetic and parasympathetic activities proposed in (37, 41).

2.5.1 Functional Interplay from the brain to the heart

The top-down functional interplay is quantified through a model of synthetic heartbeat generation based on Laguerre expansions of RR series (see Candia-Rivera et al., 2021a for further details). Briefly, heartbeat generation is based on the modulation function *m(t)*, which contains the fluctuations with respect to the baseline heart rate. Such fluctuations are modeled including the sympathetic and parasympathetic interplay. In Eq. (1), the modulation function is expressed as a linear combination of sympathetic (SAI) and parasympathetic activity index (PAI), and their respective control coefficients C_{SAI} and C_{PAI} representing the proportional central nervous system contribution:

$$m(t) = C_{SAI}(t) \cdot SAI(t) + C_{PAI}(t) \cdot PAI(t) \qquad (1)$$

The modulation function is then taken as input to an integrate-and-fire model (37). The model is fitted on the RR interval series using a 15-seconds sliding time window and a linear regression model with no constant term. Then, the interaction between heartbeat dynamics and the cortical activity is defined as:

$$SDG_{EEG\ F \rightarrow X}(t) = C_X(t) / EEG_F(t-1) \qquad (2)$$

where $X \in \{SAI, PAI\}$, and EEG_F indicates the time-varying EEG power with $F \in \{\delta, \theta, \alpha, \beta, \gamma\}$.

2.5.2 Functional Interplay from the heart to the brain

The functional interplay from heart to brain is quantified through a model based on the generation of synthetic EEG series using an adaptative Markov process (42). The model is fitted using a least-square auto-regressive process to estimate cardiac sympathovagal contributions to the ongoing fluctuations in EEG power as:

$$EEG_F(t) = \kappa_F \cdot EEG_F(t-1) + \Psi_F(t-1) + \varepsilon_F \qquad (3)$$

where F is the EEG frequency band, κ_F is a fitting constant, ε_F is the adjusted error, and Ψ_F indicates the fluctuations of EEG power in F. Then, the heart–to–brain functional coupling coefficients are calculated as follows:

$$SDG_{X \rightarrow EEG\ F}(t) = \Psi_F(t) / X(t) \qquad (4)$$

where X ∈ {SAI, PAI}. For further details, please see Candia-Rivera et al., 2022a.

The software for computation of SAI and PAI is available at *www.saipai-hrv.com*. The source code implementing the SV-SDG model is available at *www.github.com/diegocandiar/brain_heart_svsdg*.

2.6 Multivariate analysis

In order to identify the most significant brain-heart features sensitive to mental stress, a multivariate analysis was performed. The feature selection is based on the ranking provided by the computation of Minimum Redundancy Maximum Relevance (MRMR) scores (43) and was computed over the 180 SV-SDG-derived features (180 = 2 directions x 2 autonomic markers x 5 brain oscillations x 9 channels) to select the five most significant ones in two conditions: (i) a linear regression model predicting the median stress level in each condition, and (ii) a binary classification algorithm to discern low vs high stress level.

The MRMR score computation algorithm is as follows:

1. The relevance V_x of all features x is computed. The feature with the largest relevance $\max_{x \in \Omega} V_x$ is selected. The selected feature is added to an empty set of features S.
   V_x is defined as:

$$V_x = \frac{1}{|S|} \sum_{x \in S} I(x, y) \qquad (5)$$

Where $S \vee$ is the number of features in S and $I(x, y)$ is the mutual information between the feature x and the output y:

$$I(x, y) = \sum_{ij} p(x_i, y_j) log \frac{p(x_i, y_j)}{p(x_i) p(y_j)} \qquad (6)$$

2. Next, the features with non-zero relevance V_x and zero redundancy W_x in S^c (complement of S) are identified. Then, select the feature with the largest relevance, $\max_{x \in S^c, W_x = 0} V_x$. The selected feature is added to the set S.

   W_x is defined as:

$$W_x = \frac{1}{|S|^2} \sum_{x,z \in S} I(x,z) \tag{7}$$

If S^c does not include a feature with non-zero relevance and zero redundancy, skip step number 3

3. Repeat step number 2 until the redundancy W_x is not zero for all features in S^c.
4. Select the feature with the largest MIQ, with non-zero relevance and non-zero redundancy in S^c, and add the selected feature to the set S.

   MIQ is defined as:

$$\max_{x \in S^c} MIQ = \max_{x \in S^c} \frac{V_x}{W_x} = \max_{x \in S^c} \frac{I(x,y)}{\frac{1}{|S|} \sum_{z \in S} I(x,z)} \tag{8}$$

5. Repeat Step 4 until the relevance is zero for all features in S^c.
6. Add the features with zero relevance to S in random order.

The multivariate analyses are performed in a 5-fold cross-validation framework. Linear regressions to the stress level are performed using least squares kernel regression with regularization strength set to 0.027. The stress level was quantified “0” at rest, “1” for stressor 1, “4” for stressor 2, and “5” for stressor 3 to closely match the median stress ratings from subjects’ self-assessment reports. The regression performance is measured through Root Mean Squared Error (RMSE) for the prediction of median stress ratings. Binary classification for the low vs. high stress recognition was performed through a kernel naïve Bayes classifier with a Gaussian kernel, with “low stress” class associated with “rest” and “stressor 1” conditions, and “high stress” associated with the stressors 2 and 3. The classification performance is quantified through the classification accuracy.

2.7 Statistical analysis

Group-wise statistical analysis between resting state and the three stressor levels is performed through non-parametric Friedman tests, whereas two-condition comparisons are performed through Wilcoxon signed-rank test. The statistical testing was performed per EEG channel, in which the inputs correspond to SV-SDG coupling coefficient computed at different experimental conditions. The significance level of the *p*-values was corrected in accordance with the Bonferroni rule for 9 channels, with an uncorrected statistical significance set to alpha = 0.05. The samples were described group-wise using the median and related dispersion (variability) measures that was quantified though the median absolute deviation (MAD).

3 Results

The participants' self-reports on the perceived level of stress are displayed in Figure 2 for each stressful condition, where the group median ± MAD reported stress levels are 1±0, 4±1 and 5±1 ($p = 2 \cdot 10^{-14}$ from Friedman test). A multiple comparison analysis showed that the three stressful conditions are significantly different ($p<0.00005$).

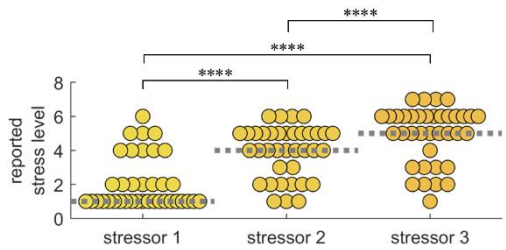

*Figure 2. Self-reported stress level for three stressful conditions. Each data point corresponds to the reported stress level per subject for each for: i) stress load condition 1: documentary, ii) stress load condition 2: documentary + digit span task, iii) stress load condition 3: documentary + digit span task + red box task. **** < 0.00005 from Wilcoxon signed-rank test.*

Cardiac autonomic activity was assessed through the sympathetic and parasympathetic activity indices (SAI and PAI, respectively). While condensing the SAI and PAI time-resolved information, median SAI and median PAI did not change significantly across the experimental conditions ($p = 0.0935$ from Friedman test on median SAI, and $p = 0.3101$ from Friedman test on median PAI). Nevertheless, SAI and PAI variability (i.e., MAD over time) significantly changes across the experimental conditions ($p = 7 \cdot 10^{-6}$ from Friedman test on SAI variability and $p = 4 \cdot 10^{-9}$ from Friedman test on PAI variability). Figure 3 depicts group-wise distributions for SAI and PAI median and variability, with evident increase in the autonomic variability in the three stressful conditions as compared to rest.

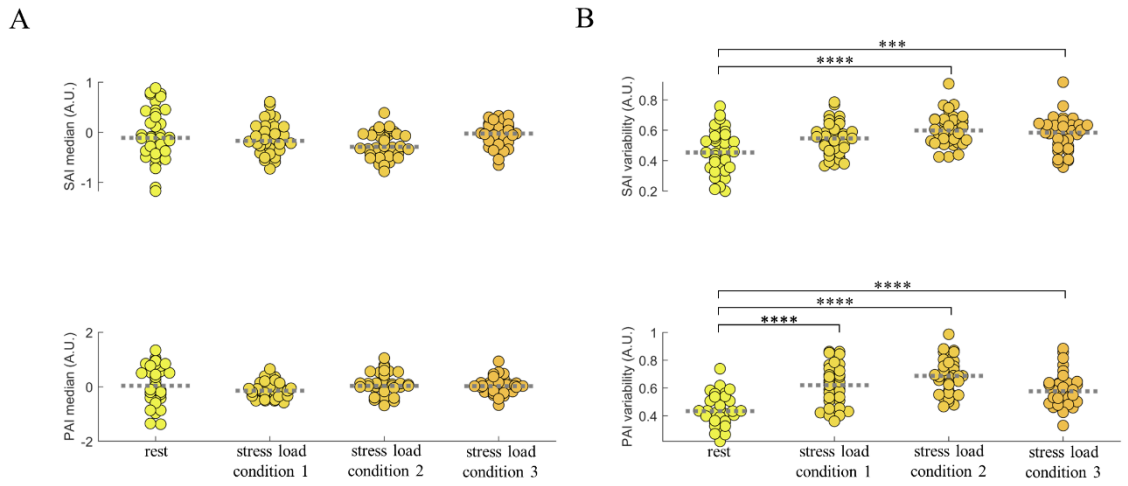

*Figure 3. Group-wise distributions of SAI and PAI median and variability for each experimental condition. Each data point corresponds to the measured autonomic marker per subject at each of the four conditions. (A) SAI and PAI median. (B) SAI and PAI variability as measured through median absolute deviation (M.A.D.). The time-varying autonomic indexes were z-score normalized for the whole experimental protocol duration before computing median and M.A.D values. ** $p < 0.005$, *** $p < 0.0005$, **** $p < 0.00005$ (Bonferroni-corrected significance at $\alpha < 0.00833$).*

Since autonomic variability is sensitive to stress levels, we further explored how they relate to brain–heart interplay. Figure 4 illustrates results from the Friedman tests on group-wise brain-heart variability changes among experimental conditions. Most of the significant changes among conditions are associated with ascending interactions, especially originating from sympathetic and vagal activity targeting EEG oscillations in the alpha band. Ascending heart-to-brain communication targeting EEG oscillations in the theta, beta and gamma bands show significant changes as well, together with descending interactions from cortical gamma oscillations to vagal activity. In contrast, cortical power variability mostly shows not significant changes, with a few statistical differences associated with gamma oscillations in the left-frontal electrodes.

For the sake of completeness, results on the median brain-heart are shown in Supplementary Figure 1. Mental stress mainly modulates heart-to-brain functional communication, especially targeting delta, alpha, beta (in the left hemisphere), and gamma bands.

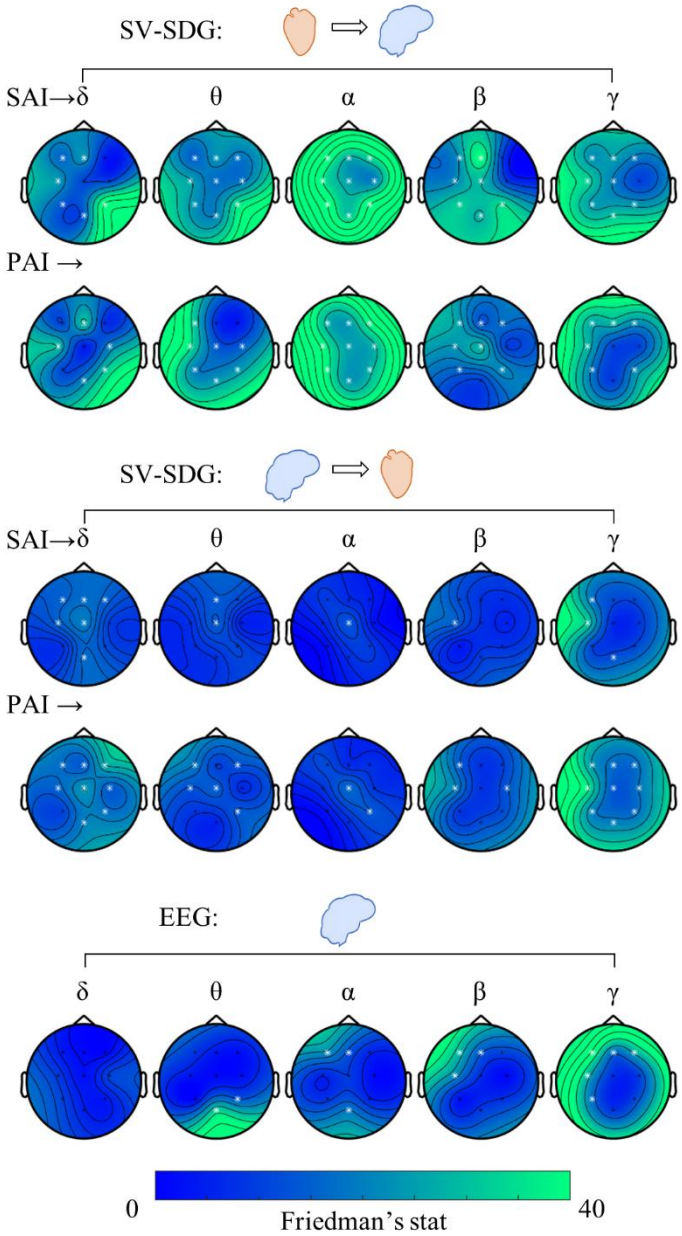

Figure 4. Friedman test on brain–heart interplay variability and EEG power variability at the four experimental conditions. Colormaps indicate the Friedman test statistic. White electrodes indicate $p < 0.0056$.

According to the MRMR algorithm, the five most informative features for the linear regression analysis and the low vs. high stress classification are reported in Table 1 and depicted in Fig. 5. In both multivariate analyses, ascending features from SAI and PAI are prevalent. To illustrate, while median stress level prediction mostly uses SAI→beta, most of the information needed for low vs high stress classification is provided by PAI→gamma.

In the regression analysis, the RMSE was 1.6851, and its output shows a significant difference between all predicted stress levels but stressor 2 vs stressor 3 (Figure 5C). In the

classification, the five brain-heart features achieved a discrimination accuracy as high as 77% (Figure 5D), with a sensitivity of 85.14% on detecting high stress, and 68.92% specificity.

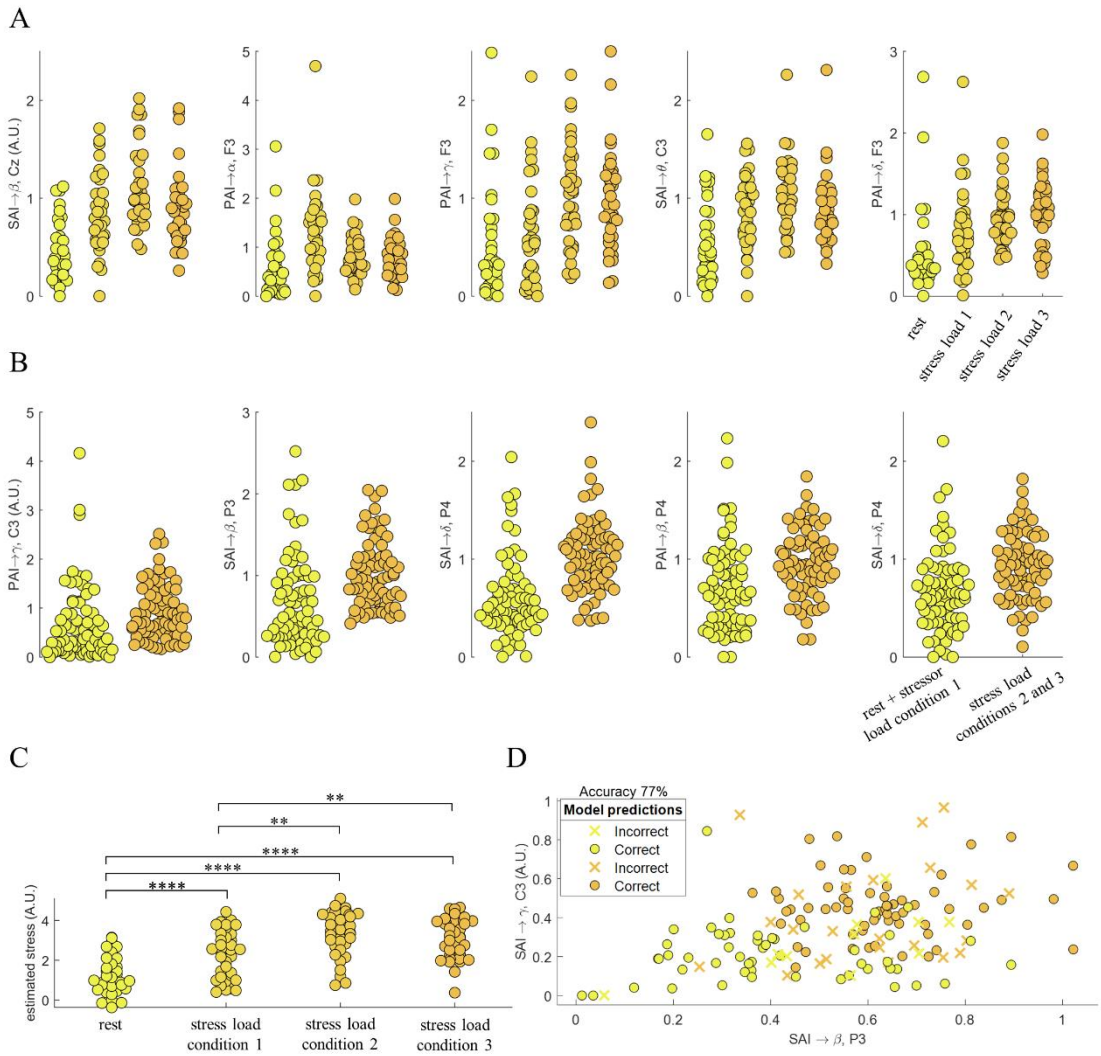

*Figure 5. (A) Best five brain–heart interplay markers to regress the stress level (regression to the group median stress level: rest=0, stressor condition 1=1, stressor condition 2=4, stressor condition 3=5). (B) Best five brain–heart interplay markers to classify low vs high stress level (low: rest + stressor1, high: stressor2 + stressor3). (C) Model output to the stress level linear regression using the best five markers under the MRMR criteria. (D) Model output to the stress level linear binary classification using the best five markers under the MRMR criteria. Yellow circles are low stress and orange circles are high stress conditions. ** $p < 0.005$, *** $p < 0.0005$, **** $p < 0.00005$ (Bonferroni-corrected significance at $\alpha < 0.00833$).*

Table 1. Minimum redundancy maximum relevance (MRMR) scores of the best five brain-heart variability markers for regression to the level of stress (rest=0, stressor condition 1=1, stressor condition 2=4, stressor condition 3=5) and for the binary classification low vs high stress (low=rest + stressor condition 1, high=stressor conditions 2 and 3).

	1st feature	2nd feature	3rd feature	4th feature	5th feature
Regression	SAI→β, Cz MRMR=0.2395	PAI→α, F3 MRMR=0.2247	PAI→γ, F3 MRMR=0.1771	SAI→θ, C3 MRMR=0.1669	PAI→δ, P4 MRMR=0.1521
Binary classification	PAI→γ, C3 MRMR=0.1464	SAI→β, P3 MRMR=0.1399	SAI→δ, P4 MRMR=0.1156	PAI→β, P4 MRMR=0.0473	SAI→δ, F3 MRMR=0.0453

Figure 6 shows exemplary SAI→beta and SAI→delta estimates from one subject for the whole duration of the experimental protocol. An overall increased variability of both markers can be observed in stressful conditions 2 and 3 with respect to rest and stressful condition 1.

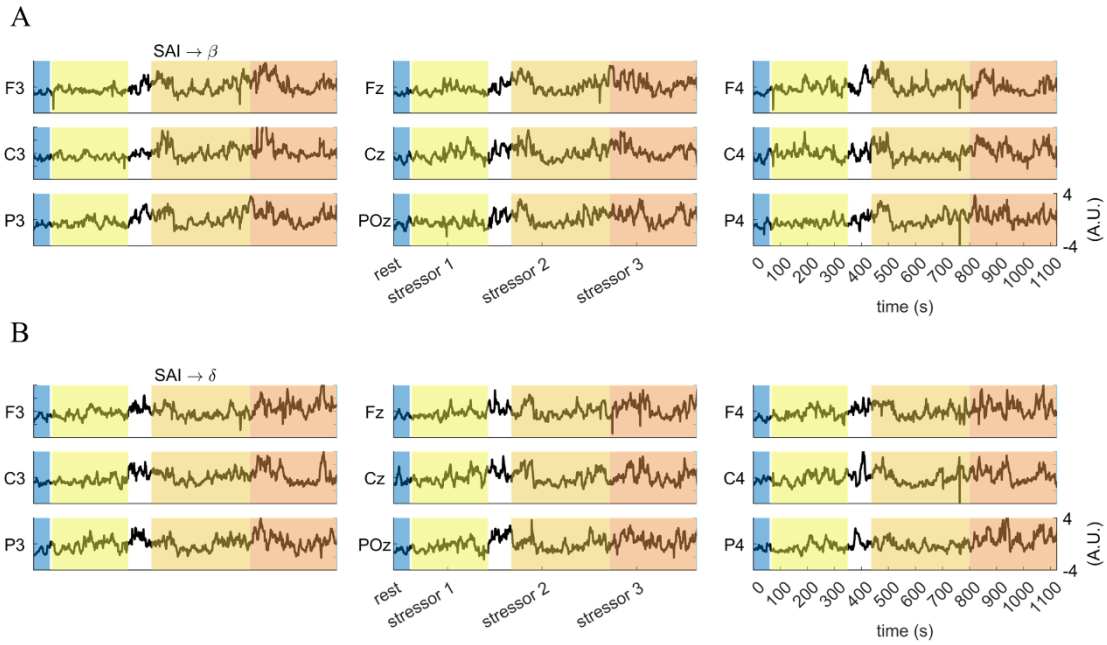

Figure 6. Exemplary participant during the experimental protocol in their fluctuations in (A) SAI→beta and (B) SAI→delta modulations.

4 Discussion

Supported by existing evidence on the physiological responses to mental stress at a central and autonomic nervous system levels (2, 10), and by linking stress to emotional responses, which are associated with functional brain–heart interplay modulation (and specifically, a directed interplay from the heart to the brain) (32, 33), we investigated functional brain–heart interplay directionally with the hypothesis of its modulation in mental stress.

When condensing the temporal dynamics of sympathetic and parasympathetic activities throughout the experimental conditions, on the one hand we observed that SAI and PAI central tendencies (median) did not change among stress levels. On the other hand, we observed that the variability (MAD) of SAI and PAI significantly increased in accordance with stress levels up to stressful condition 2. Sympathetic activity, as measured through systolic blood pressure, heart rate, ventricular ejection fraction, and skin conductance, has been associated with mental stress (17); moreover, mental stress induced by mental arithmetic increases heart rate variability power in the low frequency and a decrease in its high frequency power (44–47), suggesting an increase in the sympathetic tone, and a decrease in the parasympathetic one. Stress also modulates heartbeat non-linear dynamics (15, 48). Changes in attention have been referred to a source of autonomic variability (49). Furthermore, some studies have suggested that high frequency fluctuations in heartbeat dynamics are associated with memory retrieval, reaction time, and action execution (45, 50, 51), suggesting a dynamic interaction between sympathetic and parasympathetic activities under stress elicitation. As stress elicitation may involve some executive functions (e.g., self-control and working memory), the role of high frequency autonomic activity has been associated with specific dimensions of executive functioning (52–55).

We observed differences among stressful conditions in EEG oscillations in the gamma band. The existing evidence on EEG and stress shows heterogeneous and divergent findings with respect to frequency bands; to illustrate, some studies suggest that different dimensions of stress are associated with alpha-beta interactions (9, 46, 56), theta-beta interactions (56, 57), alpha-gamma interactions (58–60), and theta-alpha interactions (59). Such heterogeneity may be related to the subjectivity and thus high inter-subject variability on perceived stress (58), as well as to the coping strategies (61). For instance, the processing of concurrent inputs/tasks requires multiple access to the working memory (62). Another source of variability may be associated with the level of cognitive demand of the tasks, which may not be directly related to the stress level (63). In this study, the digit span task involved a verbal report, which is also associated with EEG signatures of parieto-occipital desynchronizations of lower alpha (64).

We observed EEG activity modulation as linked to both autonomic branches, whose activity was measured through SAI and PAI. Particularly, our results on brain–heart interplay shows that the variability of ascending heart–to–brain communication reflects the level of stress, especially until stressful condition 2, as compared to descending brain–to–heart modulations. Indeed, the highest stress level is not statistically associated with the highest variability of heart–to–brain modulation, nor with SAI and PAI dynamics. We speculate this may be due to the following main factors: (i) perceived stress level is mitigated or masked by mental fatigue due sustained attention (65); (ii) the increasing stress conditions may be subject to an attentional-bradycardic effect to hyper-arousing conditions (66, 67), also known as "freezing" effect, and thus highest stress conditions may be associated with a different physiological response than other stressful conditions.

Previous studies on physiological correlates of stress focused on top-down mechanisms exclusively (5, 68). While brain responses may precede cardiac responses, as measured through EEG (46, 60) and fMRI (69, 70), stressors may elicit activity in the amygdala and hippocampus such that a subsequent bottom-up control is activated (71). Indeed, brain and heart continuously influence each other (70), and the ascending arousal system shapes brain dynamics to mediate awareness of mental states (72), as well as to facilitate performance at different tasks (73, 74) and to shape physical and emotional arousal (32, 33). Stress regulation shares mechanisms involved in emotion regulation as well (29). To illustrate, anterior insula integrates interoceptive signals during emotional and cognitive processing, being these processes involved to the monitoring of the physiological state of the body (75). The neural monitoring of cardiac inputs may trigger physiological adjustments in the frame of homeostatic and allostatic regulations under emotion elicitation (31, 76). The functional brain–heart interplay under stress elicitation has been shown in heartbeat-evoked potentials correlating with stress-induced changes in cardiac output (17), and correlates of functional connectivity with heart rate variability (26). The role of cardiac inputs in the neurophysiology of stress is also supported by the experimental evidence showing an increased information flow from heart-to-brain during increased attention (49) and disrupted abilities on detecting cardiac and respiratory signals from oneself under anxiety (77, 78).

On the bottom-up modulation, we observed that both sympathetic and vagal oscillations map onto various EEG oscillations at different frequency bands. Indeed, sympathetic origin of brain-heart interplay in stress was expected because of previous evidence (13, 14, 17, 18). In this study, SAI→beta interplay seems more sensitive to changes in stress levels. The involvement of beta waves in mental stress has been previously reported (79), along with alpha-beta interactions (9, 46, 56) and theta-beta interactions (56, 57). Note that EEG oscillations in the theta band has been consistently reported as a sensitive correlate of emotion processing (80) also in a heart–to–brain communication (33). Our results show that preferential heart–to–brain communication

occur over the frontal and parietal cortical regions, consistently with previous report on stress (4) and correlates of cognitive operations (81).

We showed that a multivariate analysis helps distinguishing between stress levels, as compared to individual autonomic markers. While the use of low-density EEG in this study is certainly a limitation to understand the brain mapping and cortical dynamics of stress neurophysiology, it proves the suitability of this kind of devices to detect levels of stress with potential commercial applications. The study of mental stress elicited in other paradigms, such as mental arithmetic, could give a broader view of the physiological processes involved in brain–heart information exchange. Our study confirms the advantages of analyzing the interactions between brain and heart, instead of studying heart rate and brain dynamics exclusively (82, 83). The understanding of brain–heart dynamics and the neurophysiological substrates of stress has a clinical relevance. Heart rate variability markers are acknowledged to reflect autonomic dysregulation, which may lead to morbidity and mortality (84, 85). The evidence also shows differences in heart rate variability between healthy humans and different mood disorders, but also as a marker of the effects of antidepressant medications (84). The description of stress mechanisms can enlighten the apparent relationships with cardiac death (86), cardiovascular disease (87), sudden death (88), and psychiatric disorders (89). The evidence in other markers of brain–heart interplay shows as well that the dynamic interaction of these systems may relate to different aspects of mental health (17, 90, 91).

5 Conclusions

Stress neurophysiology comprises dynamic and bidirectional brain–body interactions, where functional bodily feedback is involved in shaping the perceived mental stress level. These results are in line with the experimental evidence showing a dynamical information exchange between central and autonomous nervous systems during emotional arousal and physical stress. Estimates of functional brain–heart interplay may be suitable biomarkers of mental stress.

6 Acknowledgements

The research leading to these results has received funding from the European Commission - Horizon 2020 Program under grant agreement n° 813234 of the project “RHUMBO”.

7 Authors’ contributions

Conceptualization: D. Candia-Rivera and T. Z. Ramsøy; Data curation: K. Norouzi; Formal analysis and Investigation: D. Candia-Rivera and G. Valenza; Methodology: D. Candia-Rivera; Supervision: T. Z. Ramsøy and G. Valenza; Writing - original draft: D. Candia-Rivera; Writing - review & editing: All authors.

References

1. **Gunnar M**, **Quevedo K**. The Neurobiology of Stress and Development. *Annual Review of Psychology* 58: 145–173, 2007. doi: 10.1146/annurev.psych.58.110405.085605.

2. **Lamotte G**, **Shouman K**, **Benarroch EE**. Stress and central autonomic network. *Autonomic Neuroscience* 235: 102870, 2021. doi: 10.1016/j.autneu.2021.102870.

3. **Godoy LD**, **Rossignoli MT**, **Delfino-Pereira P**, **Garcia-Cairasco N**, **de Lima Umeoka EH**. A Comprehensive Overview on Stress Neurobiology: Basic Concepts and Clinical Implications. *Frontiers in Behavioral Neuroscience* 12, 2018. doi: 10.3389/fnbeh.2018.00127.

4. **Ridderinkhof KR**, **Ullsperger M**, **Crone EA**, **Nieuwenhuis S**. The role of the medial frontal cortex in cognitive control. *Science* 306: 443–447, 2004. doi: 10.1126/science.1100301.

5. **Janak PH**, **Tye KM**. From circuits to behaviour in the amygdala. *Nature* 517: 284–292, 2015. doi: 10.1038/nature14188.

6. **Burgos-Robles A**, **Kimchi EY**, **Izadmehr EM**, **Porzenheim MJ**, **Ramos-Guasp WA**, **Nieh EH**, **Felix-Ortiz AC**, **Namburi P**, **Leppla CA**, **Presbrey KN**, **Anandalingam KK**, **Pagan-Rivera PA**, **Anahtar M**, **Beyeler A**, **Tye KM**. Amygdala inputs to prefrontal cortex guide behavior amid conflicting cues of reward and punishment. *Nat Neurosci* 20: 824–835, 2017. doi: 10.1038/nn.4553.

7. **Godsil BP**, **Kiss JP**, **Spedding M**, **Jay TM**. The hippocampal–prefrontal pathway: The weak link in psychiatric disorders? *European Neuropsychopharmacology* 23: 1165–1181, 2013. doi: 10.1016/j.euroneuro.2012.10.018.

8. **Katmah R**, **Al-Shargie F**, **Tariq U**, **Babiloni F**, **Al-Mughairbi F**, **Al-Nashash H**. A Review on Mental Stress Assessment Methods Using EEG Signals. *Sensors* 21: 5043, 2021. doi: 10.3390/s21155043.

9. **Vanhollebeke G**, **De Smet S**, **De Raedt R**, **Baeken C**, **van Mierlo P**, **Vanderhasselt M-A**. The neural correlates of psychosocial stress: A systematic review and meta-analysis of spectral analysis EEG studies. *Neurobiology of Stress* 18: 100452, 2022. doi: 10.1016/j.ynstr.2022.100452.

10. **Silvani A**, **Calandra-Buonaura G**, **Dampney RAL**, **Cortelli P**. Brain-heart interactions: physiology and clinical implications. *Philos Trans A Math Phys Eng Sci* 374, 2016. doi: 10.1098/rsta.2015.0181.

11. **Valenza G**, **Sclocco R**, **Duggento A**, **Passamonti L**, **Napadow V**, **Barbieri R**, **Toschi N**. The central autonomic network at rest: Uncovering functional MRI correlates of time-varying autonomic outflow. *NeuroImage* 197: 383–390, 2019. doi: 10.1016/j.neuroimage.2019.04.075.

12. **Valenza G**, **Passamonti L**, **Duggento A**, **Toschi N**, **Barbieri R**. Uncovering complex central autonomic networks at rest: a functional magnetic resonance imaging study on complex cardiovascular oscillations. *Journal of The Royal Society Interface* 17: 20190878, 2020. doi: 10.1098/rsif.2019.0878.

13. **Vrijkotte TGM**, **van Doornen LJP**, **de Geus EJC**. Effects of Work Stress on Ambulatory Blood Pressure, Heart Rate, and Heart Rate Variability. *Hypertension* 35: 880–886, 2000. doi: 10.1161/01.HYP.35.4.880.

14. **Hjortskov N**, **Rissén D**, **Blangsted AK**, **Fallentin N**, **Lundberg U**, **Søgaard K**. The effect of mental stress on heart rate variability and blood pressure during computer work. *Eur J Appl Physiol* 92: 84–89, 2004. doi: 10.1007/s00421-004-1055-z.

15. **Schubert C**, **Lambertz M**, **Nelesen RA**, **Bardwell W**, **Choi J-B**, **Dimsdale JE**. Effects of stress on heart rate complexity—A comparison between short-term and chronic stress. *Biological Psychology* 80: 325–332, 2009. doi: 10.1016/j.biopsycho.2008.11.005.

16. **Kim H-G**, **Cheon E-J**, **Bai D-S**, **Lee YH**, **Koo B-H**. Stress and Heart Rate Variability: A Meta-Analysis and Review of the Literature. *Psychiatry Investig* 15: 235–245, 2018. doi: 10.30773/pi.2017.08.17.

17. **Gray MA**, **Taggart P**, **Sutton PM**, **Groves D**, **Holdright DR**, **Bradbury D**, **Brull D**, **Critchley HD**. A cortical potential reflecting cardiac function. *Proc Natl Acad Sci USA* 104: 6818–6823, 2007. doi: 10.1073/pnas.0609509104.

18. **Greco A**, **Valenza G**, **Lazaro J**, **Garzon-Rey JM**, **Aguilo J**, **De-la-Camara C**, **Bailon R**, **Scilingo EP**. Acute stress state classification based on electrodermal activity modeling. *IEEE Transactions on Affective Computing* Early Access: 1–1, 2021. doi: 10.1109/TAFFC.2021.3055294.

19. **Boiten FA**, **Frijda NH**, **Wientjes CJE**. Emotions and respiratory patterns: review and critical analysis. *International Journal of Psychophysiology* 17: 103–128, 1994. doi: 10.1016/0167-8760(94)90027-2.

20. **Vinkers CH**, **Penning R**, **Hellhammer J**, **Verster JC**, **Klaessens JHGM**, **Olivier B**, **Kalkman CJ**. The effect of stress on core and peripheral body temperature in humans. *Stress* 16: 520–530, 2013. doi: 10.3109/10253890.2013.807243.

21. **Nakamura K**, **Morrison SF**. Central sympathetic network for thermoregulatory responses to psychological stress. *Autonomic Neuroscience* 237: 102918, 2022. doi: 10.1016/j.autneu.2021.102918.

22. **Collins SM**. IV. Modulation of intestinal inflammation by stress: basic mechanisms and clinical relevance. *American Journal of Physiology-Gastrointestinal and Liver Physiology* 280: G315–G318, 2001. doi: 10.1152/ajpgi.2001.280.3.G315.

23. **Söderholm JD**, **Perdue MH**. II. Stress and intestinal barrier function. *American Journal of Physiology-Gastrointestinal and Liver Physiology* 280: G7–G13, 2001. doi: 10.1152/ajpgi.2001.280.1.G7.

24. **Ulrich-Lai YM**, **Herman JP**. Neural regulation of endocrine and autonomic stress responses. *Nat Rev Neurosci* 10: 397–409, 2009. doi: 10.1038/nrn2647.

25. **Segerstrom SC**, **Miller GE**. Psychological Stress and the Human Immune System: A Meta-Analytic Study of 30 Years of Inquiry. *Psychological Bulletin* 130: 601–630, 2004. doi: 10.1037/0033-2909.130.4.601.

26. **Chand T**, **Li M**, **Jamalabadi H**, **Wagner G**, **Lord A**, **Alizadeh S**, **Danyeli LV**, **Herrmann L**, **Walter M**, **Sen ZD**. Heart Rate Variability as an Index of Differential Brain Dynamics at Rest and After Acute Stress Induction. *Front Neurosci* 14: 645, 2020. doi: 10.3389/fnins.2020.00645.

27. **Pernice R**, **Antonacci Y**, **Zanetti M**, **Busacca A**, **Marinazzo D**, **Faes L**, **Nollo G**. Multivariate Correlation Measures Reveal Structure and Strength of Brain–Body

Physiological Networks at Rest and During Mental Stress. *Frontiers in Neuroscience* 14: 1427, 2021. doi: 10.3389/fnins.2020.602584.

28. **McEwen BS**. Physiology and Neurobiology of Stress and Adaptation: Central Role of the Brain. *Physiological Reviews* 87: 873–904, 2007. doi: 10.1152/physrev.00041.2006.

29. **Thayer JF**, **Mather M**, **Koenig J**. Stress and aging: A neurovisceral integration perspective. *Psychophysiology* 58: e13804, 2021. doi: 10.1111/psyp.13804.

30. **Kreibig SD**. Autonomic nervous system activity in emotion: A review. *Biological Psychology* 84: 394–421, 2010. doi: 10.1016/j.biopsycho.2010.03.010.

31. **Pace-Schott EF**, **Amole MC**, **Aue T**, **Balconi M**, **Bylsma LM**, **Critchley H**, **Demaree HA**, **Friedman BH**, **Gooding AEK**, **Gosseries O**, **Jovanovic T**, **Kirby LAJ**, **Kozlowska K**, **Laureys S**, **Lowe L**, **Magee K**, **Marin M-F**, **Merner AR**, **Robinson JL**, **Smith RC**, **Spangler DP**, **Van Overveld M**, **VanElzakker MB**. Physiological feelings. *Neuroscience & Biobehavioral Reviews* 103: 267–304, 2019. doi: 10.1016/j.neubiorev.2019.05.002.

32. **Candia-Rivera D**, **Catrambone V**, **Barbieri R**, **Valenza G**. Functional assessment of bidirectional cortical and peripheral neural control on heartbeat dynamics: a brain-heart study on thermal stress. *NeuroImage* 251: 119023, 2022. doi: 10.1016/j.neuroimage.2022.119023.

33. **Candia-Rivera D**, **Catrambone V**, **Thayer JF**, **Gentili C**, **Valenza G**. Cardiac sympathetic-vagal activity initiates a functional brain-body response to emotional arousal. *Proceedings of the National Academy of Sciences* , 2022. doi: https://doi.org/10.1073/pnas.2119599119.

34. **Füstös J**, **Gramann K**, **Herbert BM**, **Pollatos O**. On the embodiment of emotion regulation: interoceptive awareness facilitates reappraisal. *Social Cognitive and Affective Neuroscience* 8: 911–917, 2013. doi: 10.1093/scan/nss089.

35. **Klein AS**, **Dolensek N**, **Weiand C**, **Gogolla N**. Fear balance is maintained by bodily feedback to the insular cortex in mice. *Science* 374: 1010–1015, 2021. doi: 10.1126/science.abj8817.

36. **Schulz A**, **Vögele C**. Interoception and stress. *Frontiers in Psychology* 6: 993, 2015. doi: 10.3389/fpsyg.2015.00993.

37. **Candia-Rivera D**, **Catrambone V**, **Barbieri R**, **Valenza G**. Integral pulse frequency modulation model driven by sympathovagal dynamics: Synthetic vs. real heart rate variability. *Biomedical Signal Processing and Control* 68: 102736, 2021. doi: 10.1016/j.bspc.2021.102736.

38. **Oostenveld R**, **Fries P**, **Maris E**, **Schoffelen J-M**. FieldTrip: Open Source Software for Advanced Analysis of MEG, EEG, and Invasive Electrophysiological Data. *Computational Intelligence and Neuroscience* 2011: 9 pages, 2011. doi: 10.1155/2011/156869.

39. **Candia-Rivera D**, **Catrambone V**, **Valenza G**. The role of electroencephalography electrical reference in the assessment of functional brain–heart interplay: From methodology to user guidelines. *Journal of Neuroscience Methods* 360: 109269, 2021. doi: 10.1016/j.jneumeth.2021.109269.

40. **Citi L**, **Brown EN**, **Barbieri R**. A Real-Time Automated Point Process Method for Detection and Correction of Erroneous and Ectopic Heartbeats. *IEEE Trans Biomed Eng* 59: 2828–2837, 2012. doi: 10.1109/TBME.2012.2211356.

41. **Valenza G**, **Citi L**, **Saul JP**, **Barbieri R**. Measures of sympathetic and parasympathetic autonomic outflow from heartbeat dynamics. *Journal of Applied Physiology* 125: 19–39, 2018. doi: 10.1152/japplphysiol.00842.2017.

42. **Al-Nashash H**, **Al-Assaf Y**, **Paul J**, **Thakor N**. EEG signal modeling using adaptive Markov process amplitude. *IEEE Transactions on Biomedical Engineering* 51: 744–751, 2004. doi: 10.1109/TBME.2004.826602.

43. **Peng H**, **Long F**, **Ding C**. Feature Selection Based on Mutual Information: Criteria of Max-Dependency, Max-Relevance, and Min-Redundancy. *IEEE Transactions on Pattern Analysis and Machine Intelligence* 27: 1226–1238, 2005. doi: 10.1109/TPAMI.2005.159.

44. **Dzhebrailova TD**, **Korobeinikova II**, **Karatygin NA**, **Dudnik EN**. Dynamics of EEG α activity and heart rate variability in subjects performing cognitive tests. *Hum Physiol* 41: 599–610, 2015. doi: 10.1134/S0362119715040076.

45. **Wang X**, **Liu B**, **Xie L**, **Yu X**, **Li M**, **Zhang J**. Cerebral and neural regulation of cardiovascular activity during mental stress. *BioMedical Engineering OnLine* 15: 160, 2016. doi: 10.1186/s12938-016-0255-1.

46. **Yu X**, **Zhang J**, **Xie D**, **Wang J**, **Zhang C**. Relationship between scalp potential and autonomic nervous activity during a mental arithmetic task. *Autonomic Neuroscience* 146: 81–86, 2009. doi: 10.1016/j.autneu.2008.12.005.

47. **Yu X**, **Zhang J**. Estimating the cortex and autonomic nervous activity during a mental arithmetic task. *Biomedical Signal Processing and Control* 7: 303–308, 2012. doi: 10.1016/j.bspc.2011.06.001.

48. **Delliaux S**, **Delaforge A**, **Deharo J-C**, **Chaumet G**. Mental Workload Alters Heart Rate Variability, Lowering Non-linear Dynamics [Online]. *Frontiers in Physiology* 10, 2019. https://www.frontiersin.org/article/10.3389/fphys.2019.00565 [12 Apr. 2022].

49. **Kumar M**, **Singh D**, **Deepak KK**. Identifying heart-brain interactions during internally and externally operative attention using conditional entropy. *Biomedical Signal Processing and Control* 57: 101826, 2020. doi: 10.1016/j.bspc.2019.101826.

50. **Hansen AL**, **Johnsen BH**, **Thayer JF**. Vagal influence on working memory and attention. *International Journal of Psychophysiology* 48: 263–274, 2003. doi: 10.1016/S0167-8760(03)00073-4.

51. **Salvia E**, **Guillot A**, **Collet C**. The Effects of Mental Arithmetic Strain on Behavioral and Physiological Responses. *Journal of Psychophysiology* 27: 173–184, 2013. doi: 10.1027/0269-8803/a000102.

52. **Duschek S**, **Muckenthaler M**, **Werner N**, **Reyes del Paso GA**. Relationships between features of autonomic cardiovascular control and cognitive performance. *Biological Psychology* 81: 110–117, 2009. doi: 10.1016/j.biopsycho.2009.03.003.

53. **Thayer JF**, **Hansen AL**, **Saus-Rose E**, **Johnsen BH**. Heart rate variability, prefrontal neural function, and cognitive performance: the neurovisceral integration perspective on self-regulation, adaptation, and health. *Ann Behav Med* 37: 141–153, 2009. doi: 10.1007/s12160-009-9101-z.

54. **Williams PG**, **Cribbet MR**, **Tinajero R**, **Rau HK**, **Thayer JF**, **Suchy Y**. The association between individual differences in executive functioning and resting high-frequency heart

rate variability. *Biological Psychology* 148: 107772, 2019. doi: 10.1016/j.biopsycho.2019.107772.

55. **Magnon V**, **Vallet GT**, **Benson A**, **Mermillod M**, **Chausse P**, **Lacroix A**, **Bouillon-Minois J-B**, **Dutheil F**. Does heart rate variability predict better executive functioning? A systematic review and meta-analysis. *Cortex* 155: 218–236, 2022. doi: 10.1016/j.cortex.2022.07.008.

56. **Wen TY**, **Aris SAM**. Electroencephalogram (EEG) stress analysis on alpha/beta ratio and theta/beta ratio. *Indonesian Journal of Electrical Engineering and Computer Science* 17: 175–182, 2020. doi: 10.11591/ijeecs.v17.i1.pp175-182.

57. **Putman P**, **Verkuil B**, **Arias-Garcia E**, **Pantazi I**, **van Schie C**. EEG theta/beta ratio as a potential biomarker for attentional control and resilience against deleterious effects of stress on attention. *Cogn Affect Behav Neurosci* 14: 782–791, 2014. doi: 10.3758/s13415-013-0238-7.

58. **Luijcks R**, **Vossen CJ**, **Hermens HJ**, **Os J van**, **Lousberg R**. The Influence of Perceived Stress on Cortical Reactivity: A Proof-Of-Principle Study. *PLOS ONE* 10: e0129220, 2015. doi: 10.1371/journal.pone.0129220.

59. **Micheloyannis S**, **Sakkalis V**, **Vourkas M**, **Stam CJ**, **Simos PG**. Neural networks involved in mathematical thinking: evidence from linear and non-linear analysis of electroencephalographic activity. *Neuroscience Letters* 373: 212–217, 2005. doi: 10.1016/j.neulet.2004.10.005.

60. **Umeno K**, **Hori E**, **Tabuchi E**, **Takakura H**, **Miyamoto K**, **Ono T**, **Nishijo H**. Gamma-band EEGs predict autonomic responses during mental arithmetic. *NeuroReport* 14: 477–480, 2003.

61. **Hinault T**, **Lemaire P**. What does EEG tell us about arithmetic strategies? A review. *International Journal of Psychophysiology* 106: 115–126, 2016. doi: 10.1016/j.ijpsycho.2016.05.006.

62. **Kim C**, **Johnson NF**, **Gold BT**. Conflict adaptation in prefrontal cortex: Now you see it, now you don't. *Cortex* 50: 76–85, 2014. doi: 10.1016/j.cortex.2013.08.011.

63. **Fink A**, **Grabner RH**, **Neuper C**, **Neubauer AC**. EEG alpha band dissociation with increasing task demands. *Cognitive Brain Research* 24: 252–259, 2005. doi: 10.1016/j.cogbrainres.2005.02.002.

64. **Grabner RH**, **De Smedt B**. Neurophysiological evidence for the validity of verbal strategy reports in mental arithmetic. *Biological Psychology* 87: 128–136, 2011. doi: 10.1016/j.biopsycho.2011.02.019.

65. **Xiao Y**, **Ma F**, **Lv Y**, **Cai G**, **Teng P**, **Xu F**, **Chen S**. Sustained Attention is Associated with Error Processing Impairment: Evidence from Mental Fatigue Study in Four-Choice Reaction Time Task. *PLOS ONE* 10: e0117837, 2015. doi: 10.1371/journal.pone.0117837.

66. **Bradley MM**, **Codispoti M**, **Cuthbert BN**, **Lang PJ**. Emotion and motivation I: Defensive and appetitive reactions in picture processing. *Emotion* 1: 276–298, 2001. doi: 10.1037/1528-3542.1.3.276.

67. **Valenza G**, **Greco A**, **Gentili C**, **Lanata A**, **Sebastiani L**, **Menicucci D**, **Gemignani A**, **Scilingo EP**. Combining electroencephalographic activity and instantaneous heart rate for assessing brain–heart dynamics during visual emotional elicitation in healthy subjects.

Philosophical Transactions of the Royal Society A: Mathematical, Physical and Engineering Sciences 374: 20150176, 2016. doi: 10.1098/rsta.2015.0176.

68. **Radley J**, **Morilak D**, **Viau V**, **Campeau S**. Chronic stress and brain plasticity: mechanisms underlying adaptive and maladaptive changes and implications for stress-related CNS disorders. *Neurosci Biobehav Rev* 58: 79–91, 2015. doi: 10.1016/j.neubiorev.2015.06.018.

69. **Iacovella V**, **Faes L**, **Hasson U**. Task-induced deactivation in diverse brain systems correlates with interindividual differences in distinct autonomic indices. *Neuropsychologia* 113: 29–42, 2018. doi: 10.1016/j.neuropsychologia.2018.03.005.

70. **Pfurtscheller G**, **Blinowska KJ**, **Kaminski M**, **Schwerdtfeger AR**, **Rassler B**, **Schwarz G**, **Klimesch W**. Processing of fMRI-related anxiety and bi-directional information flow between prefrontal cortex and brain stem. *Sci Rep* 11: 22348, 2021. doi: 10.1038/s41598-021-01710-8.

71. **Arnsten AFT**. Stress signalling pathways that impair prefrontal cortex structure and function. *Nat Rev Neurosci* 10: 410–422, 2009. doi: 10.1038/nrn2648.

72. **Munn BR**, **Müller EJ**, **Wainstein G**, **Shine JM**. The ascending arousal system shapes neural dynamics to mediate awareness of cognitive states. *Nat Commun* 12: 6016, 2021. doi: 10.1038/s41467-021-26268-x.

73. **Fujimoto A**, **Murray EA**, **Rudebeck PH**. Interaction between decision-making and interoceptive representations of bodily arousal in frontal cortex. *PNAS* 118, 2021. doi: 10.1073/pnas.2014781118.

74. **Skora LI**, **Livermore JJA**, **Roelofs K**. The functional role of cardiac activity in perception and action. *Neuroscience & Biobehavioral Reviews* 137: 104655, 2022. doi: 10.1016/j.neubiorev.2022.104655.

75. **Craig AD**. How do you feel — now? The anterior insula and human awareness. *Nature Reviews Neuroscience* 10: 59–70, 2009. doi: 10.1038/nrn2555.

76. **Barrett LF**, **Simmons WK**. Interoceptive predictions in the brain. *Nat Rev Neurosci* 16: 419–429, 2015. doi: 10.1038/nrn3950.

77. **Garfinkel SN**, **Manassei MF**, **Hamilton-Fletcher G**, **In den Bosch Y**, **Critchley HD**, **Engels M**. Interoceptive dimensions across cardiac and respiratory axes. *Philosophical Transactions of the Royal Society B: Biological Sciences* 371: 20160014, 2016. doi: 10.1098/rstb.2016.0014.

78. **Harrison OK**, **Köchli L**, **Marino S**, **Luechinger R**, **Hennel F**, **Brand K**, **Hess AJ**, **Frässle S**, **Iglesias S**, **Vinckier F**, **Petzschner FH**, **Harrison SJ**, **Stephan KE**. Interoception of breathing and its relationship with anxiety. *Neuron* 109: 4080-4093.e8, 2021. doi: 10.1016/j.neuron.2021.09.045.

79. **Hayashi T**, **Okamoto E**, **Nishimura H**, **Mizuno-Matsumoto Y**, **Ishii R**, **Ukai S**. Beta Activities in EEG Associated with Emotional Stress. *International Journal of Intelligent Computing in Medical Sciences & Image Processing* 3: 57–68, 2009. doi: 10.1080/1931308X.2009.10644171.

80. **Bekkedal MYV**, **Rossi J**, **Panksepp J**. Human brain EEG indices of emotions: Delineating responses to affective vocalizations by measuring frontal theta event-related

synchronization. *Neuroscience & Biobehavioral Reviews* 35: 1959–1970, 2011. doi: 10.1016/j.neubiorev.2011.05.001.

81. **Gruber O**, **Indefrey P**, **Steinmetz H**, **Kleinschmidt A**. Dissociating Neural Correlates of Cognitive Components in Mental Calculation. *Cerebral Cortex* 11: 350–359, 2001. doi: 10.1093/cercor/11.4.350.

82. **Azzalini D**, **Rebollo I**, **Tallon-Baudry C**. Visceral Signals Shape Brain Dynamics and Cognition. *Trends in Cognitive Sciences* 23: 488–509, 2019. doi: 10.1016/j.tics.2019.03.007.

83. **Candia-Rivera D**. Brain-heart interactions in the neurobiology of consciousness. *Current Research in Neurobiology* 3: 100050, 2022. doi: 10.1016/j.crneur.2022.100050.

84. **Kemp AH**, **Quintana DS**. The relationship between mental and physical health: Insights from the study of heart rate variability. *International Journal of Psychophysiology* 89: 288–296, 2013. doi: 10.1016/j.ijpsycho.2013.06.018.

85. **Samuels MA**. The Brain–Heart Connection. *Circulation* 116: 77–84, 2007. doi: 10.1161/CIRCULATIONAHA.106.678995.

86. **Critchley HD**, **Taggart P**, **Sutton PM**, **Holdright DR**, **Batchvarov V**, **Hnatkova K**, **Malik M**, **Dolan RJ**. Mental stress and sudden cardiac death: asymmetric midbrain activity as a linking mechanism. *Brain* 128: 75–85, 2005. doi: 10.1093/brain/awh324.

87. **Hering D**, **Lachowska K**, **Schlaich M**. Role of the Sympathetic Nervous System in Stress-Mediated Cardiovascular Disease. *Curr Hypertens Rep* 17: 80, 2015. doi: 10.1007/s11906-015-0594-5.

88. **La Rovere MT**, **Gorini A**, **Schwartz PJ**. Stress, the autonomic nervous system, and sudden death. *Autonomic Neuroscience* 237: 102921, 2022. doi: 10.1016/j.autneu.2021.102921.

89. **Gurel NZ**, **Hadaya J**, **Ardell JL**. Stress-related dysautonomias and neurocardiology-based treatment approaches. *Autonomic Neuroscience* 239: 102944, 2022. doi: 10.1016/j.autneu.2022.102944.

90. **Catrambone V**, **Messerotti Benvenuti S**, **Gentili C**, **Valenza G**. Intensification of functional neural control on heartbeat dynamics in subclinical depression. *Translational Psychiatry* 11: 1–10, 2021. doi: 10.1038/s41398-021-01336-4.

91. **Iseger TA**, **Bueren NER van**, **Kenemans JL**, **Gevirtz R**, **Arns M**. A frontal-vagal network theory for Major Depressive Disorder: Implications for optimizing neuromodulation techniques. *Brain Stimulation: Basic, Translational, and Clinical Research in Neuromodulation* 13: 1–9, 2020. doi: 10.1016/j.brs.2019.10.006.